J Electroceram (2008) 21:719–723
DOI 10.1007/s10832-007-9257-5

Investigation of the cationic distribution within the lattice of a series of niobates with tetragonal tungsten bronze structure

A. Lahmar · M. Zriouil · H. Ehrenberg · E. Antic-Fidancev · S. Ganschow · B. Elouadi

Published online: 28 September 2007

Abstract Single Crystals of the series $K_3Sr_2LnNb_{10}O_{30}$ (Ln=Lanthanide) have been grown by two different techniques: micro-pulling down and solid state growth. The cationic distribution within the three large cavities of the lattice, determined from the crystal structure resolution, shows that the crystal-chemical formula is depending on the route of preparation. A spectroscopic study has evidenced a broadening of the emission peaks which is also compatible with a disorder distribution of Ln^{3+} ions over 12- and 15-fold cavities.

A. Lahmar · B. Elouadi (✉)
Laboratoire d'Elaboration, Analyse Chimique et Ingénierie des Matériaux (LEACIM), Université de La Rochelle,
avenue Michel Crépeau,
17042 La Rochelle Cedex 01, France
e-mail: belouadi@univ-lr.fr

A. Lahmar · M. Zriouil
Applied Solid State Chemistry Laboratory, Faculty of Sciences,
Charia Ibn Batota,
B. P. 1014, Rabat, Morocco

H. Ehrenberg
Institute for Complex Materials, IFW Dresden,
Helmholtzstr. 20,
01069 Dresden, Germany

E. Antic-Fidancev
Laboratoire de Chimie Appliquée de l'Etat Solide ENSCP,
Matériaux Inorganiques (CNRS UMR 7574),
11, rue P. et M. Curie,
75231 Paris Cedex 05, France

S. Ganschow
Institut für Kristallzüchtung,
Max Born-Strasse. 2,
12489 Berlin, Germany

Keywords Niobates · Tetragonal tungsten bronze structure · Crystal growth · Ceramic sintering · μ-Pulling down · Luminescence

1 Introduction

A large number of ferroelectric oxides with tetragonal tungsten bronze structural type have already been recognised as capable of endorsing properties with potential applications in different fields [1–6]. It has also been observed that some rare-earth doped compounds are of interest regarding to their diffuse phase transition for dielectric application and due to the green and blue emission light for laser technology [7–9]. However, in relation with the latter application, it should be also noted that various studies have evidenced difficulties to elaborate large single crystals for various reasons: crystal defects, incommensurate phase transitions, absence of very precise structural data, etc. The present study concerns the preparation and the structural analysis of single crystals using two-different methods. Their crystal structures were resolved with the aim to evaluate the effect of the cationic distribution (particularly rare earth ion) on the materials physical properties like luminescence and ferroelectricity. The optical investigation of Nd^{3+} and Eu^{3+} as a structural probe in these compounds was carried out with the view of a cationic disorder revelation within the corresponding composition.

2 Experimental procedure

Most of the single crystals of the series $K_3Sr_2LnNb_{10}O_{30}$ were elaborated by solid state technique but some of them

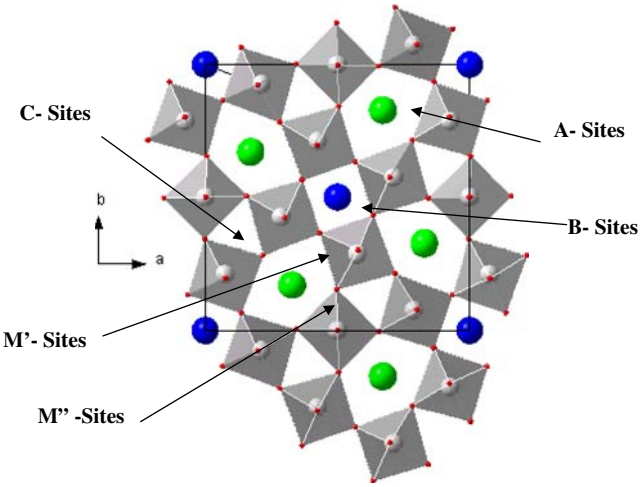

Fig. 1 View of $K_3Sr_2LnNb_{10}O_{30}$ (Ln=Lanthanide) crystal structure along [001]

(Ln=Nd, Eu) have been grown using two-different techniques: the ceramic sintering (CSM: in this work) and the micro pulling down (μPDM) methods [10]. The description of the crystal growth and the experimental set-up has been reported elsewhere (Lahmar et al., to be published).

Emission spectra of Nd^{3+} were recorded using a CwTi: Saphire laser (Coherent 890) pumped with 7w coherent argon ion laser. The spectral Analysis was made by an ARC spectra Pro-7510 monochromator using a detector of PbS cell cooled with liquid nitrogen. In the case of Eu^{3+} ions, the luminescence was recorded with Ne-lamp as exciting source. An intensified optical multichannel analyser (OMA) was used for the detection of the fluorescence.

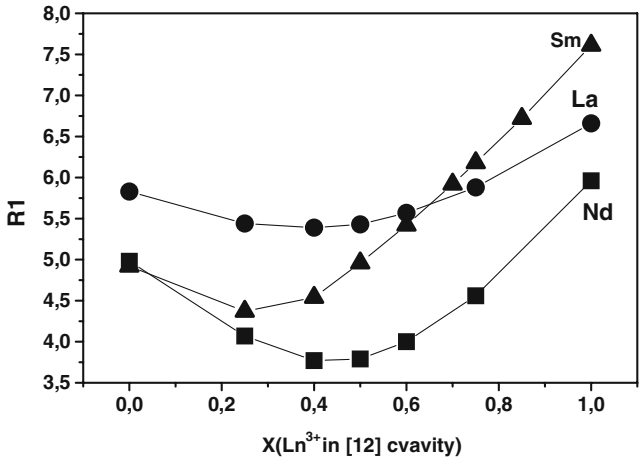

Fig. 2 Typical examples of the variation of the reliability factor (R1) versus the occupation ratio of 12-fold sites by Ln^{3+} ions at 300 K

Table 1 Crystal chemical data for the series $K_3Sr_2LnNb_{10}O_{30}$ (Ln=Nd, Eu).

General formula	Technique of synthesis	Crystal chemical formula	Lattice parameters $a=b$, c (Å) and volume V (Å^3)	
			T= 300 K	T= 122 K
$K_3Sr_2NdNb_{10}O_{30}$	Ceramic Sintering	$(K_3Sr_{0.5}\ Nd_{0.5})\ (Sr_{1.5}Nd_{0.5})Nb_{10}O_{30}$	$a=b$=12.438 (2) c=3.8929 (9) V=602.2	$a=b$=12.414 (2) c=3.8922 (5) V=599.9 (1)
	μ- Pulling down	$(K_3Sr_{0.25}\ Nd_{0.75})\ (Sr_{1.75}Nd_{0.25})Nb_{10}O_{30}$	$a=b$=12.455(9) c=3.899 (6) V=604.9(1)	$a=b$=12.434(1) c=3.9146 (8) V=603.6 (1)
$K_3Sr_2EuNb_{10}O_{30}$	Ceramic Sintering	$(K_3Sr_{0.7}\ Eu_{0.3})\ (Sr_{1.3}Eu_{0.7})Nb_{10}O_{30}$	$a=b$=12.435 (1) c=3.9030 (6) V=603.5 (1)	$a=b$=12.425 (1) c=3.9016 (5) V=602.3 (1)
	μ- Pulling down	$(K_3Sr_{0.45}\ Eu_{0.55})\ (Sr_{1.55}Eu_{0.45})Nb_{10}O_{30}$	$a=b$=12.4558 (5) c=3.9146 (5) V=607.3 (1)	$a=b$=12.4288 (6) c=3.9161 (3) V=604.9 (1)

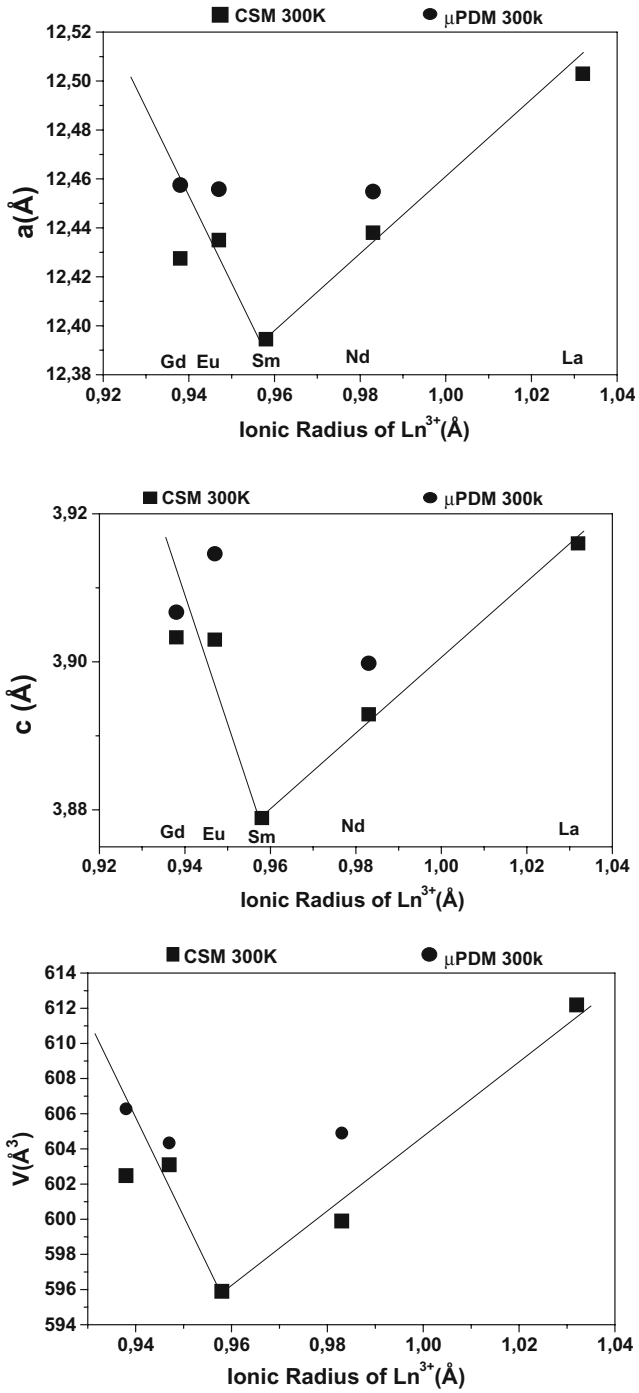

Fig. 3 Variation of the lattice parameters versus ionic radius $r_{(Ln3+)}$ for $K_3Sr_2LnNb_{10}O_{30}$ at 300 K

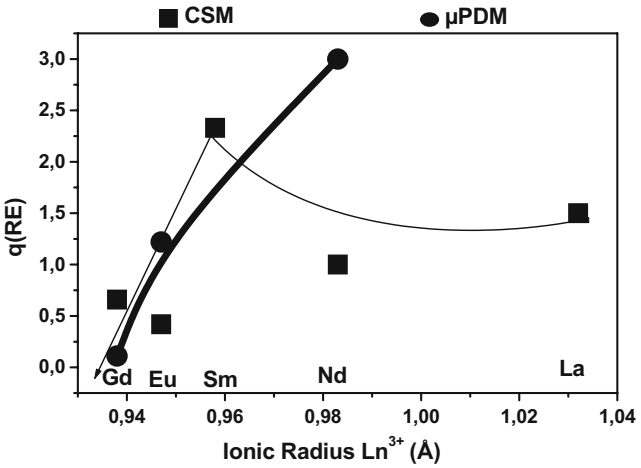

Fig. 4 Variation of the ratio [q (RE)=([15]/[12])] versus the ionic radius $r_{(Ln3+)}$ for the system $K_3Sr_2LnNb_{10}O_{30}$

3 Results and discussion

3.1 Structural analysis

The structures were refined in the space group P4/mbm. The framework of $K_3Sr_2LnNb_{10}O_{30}$ (Ln=Lanthanide) is shown in Fig. 1. The structure is made of [NbO_6] octahedra sharing apices along the c-axis and arranged in the manner to give rise to three types of cavities: A, B and C with penta-, tetra- and trigonal sections respectively. The -A sites are occupied by three different cations, K^+, Sr^{2+} and Ln^{3+} while B cavities are only filled by Sr^{2+} and Ln^{3+}. Indeed all C-sites are totally void and all octahedral cavities are occupied by Nb^{5+} ions since M′=M″=Nb. All investigated compounds are found to crystallise with the tetragonal tungsten bronze structural type represented in Fig. 1.

Despite the fact that the empirical formula is the same for all grown crystals whereas the cationic distribution over the 12- and 15-fold sites is different. Furthermore, the crystal chemical formula is deduced from the plot of the reliability factor (R1) versus rare earth distribution over these two cavities, as shown in Fig. 2. As a matter of fact, the minimum values of R1 have allowed to determine the crystal chemical formulas given in Table 1. From these results we can conclude that the temperature of the structure resolution has almost no influence on the cationic distribution, but the latter is widely dependent on two main

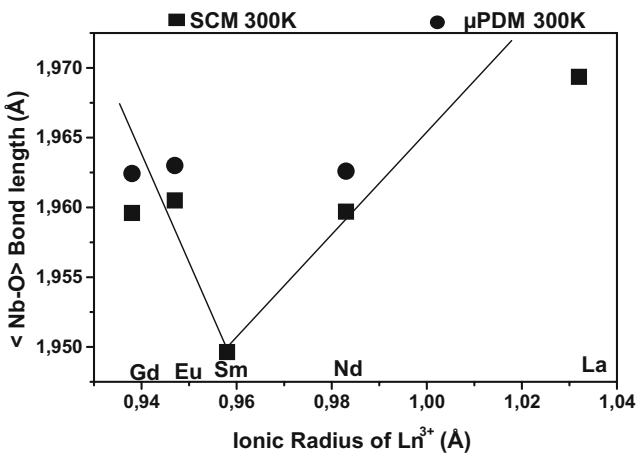

Fig. 5 Variation of <Nb–O> bond length versus the ionic radius $r_{(Ln3+)}$ for the system $K_3Sr_2LnNb_{10}O_{30}$

parameters: (1) the method of synthesis; (2) the nature of rare earth cations. Figure 3 represents the variation of the lattice parameters versus ionic radius $r_{(Ln^{3+})}$. It appears that a, c and V of the crystals grown by the μ-pulling down technique, which is a rapid method, are slightly higher than those elaborated by Ceramic Sintering Method. The plots of the ratio of rare earth ions concentration in 15-fold and 12-fold sites, respectively, [q (RE)=([15]/[12])] versus $r_{(Ln3+)}$ are given in Fig. 4. They show that for the crystals grown by the μ-pulling down method, q (RE) increases with increasing ionic radius of Ln^{3+} ions, indicating that the pentagonal cavity is more likely occupied by big lanthanide cations. In the contrary, no specific site has been detected for Ln^{3+} ions in crystals elaborated by ceramic sintering technique. This specific behaviour can probably be explained because firing at the sintering temperature for a long time tends to stabilise ordered cationic distribution.

The average variation of the bond length <Nb(1)–O> with the ionic radius $r_{(Ln^{3+})}$ is presented in Fig. 5. The Nb (1)–O average distance is situated in the range 1.95–1.97 Å. This value is shorter than the sum ($r_{(Nb^{+5})}+r_{(O^{2-})}$=2.04 Å [11]) indicating the tendency for a covalent character in this family of bonds. On the other hand, the Nb–O average length shows a minimum corresponding to the Sm phase, which appears as having the highest covalent character in this series of mixed cation niobates.

3.2 Preliminary spectroscopic investigations

The Nd^{3+} emission spectra of $K_3Sr_2NdNb_{10}O_{30}$ crystal corresponding to the $^4F_{3/2}\rightarrow{}^4I_{9/2}$ transition are given in Fig. 6. In fact, we expect to get five lines for each Nd^{3+} sites corresponding to Stark levels of $^4I_{9/2,}$ but only three broad peaks are observed, similarly to the glasses or disordered structure [12]. This broadening can be attributed

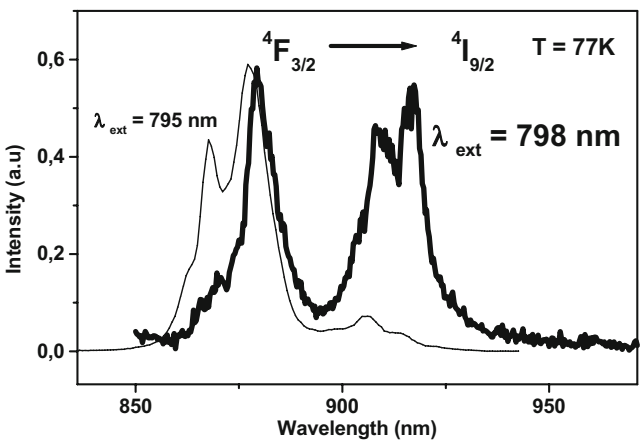

Fig. 6 Nd^{3+} Fluorescence spectra for $^4F_{3/2}\rightarrow{}^4I_{9/2}$ transition at 77 K for two excitation wavelength

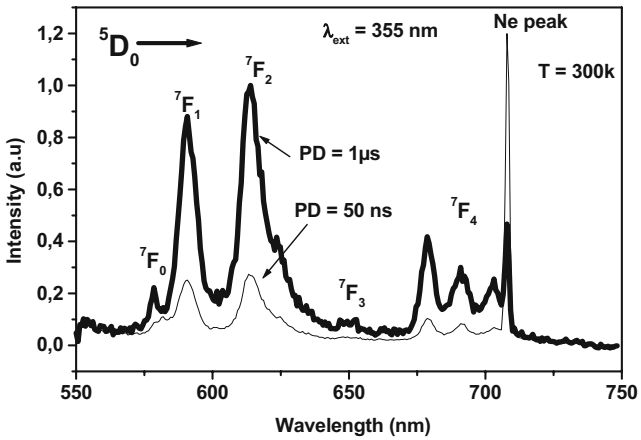

Fig. 7 Emission spectra of Eu^{3+} in $K_3Sr_2EuNb_{10}O_{30}$ crystal recorded after 50 ns (PD=50 ns, *bold plot*) and 1 μs (PD=1 μs, *light plot*)

to different emitting levels. However, on changing slightly the excitation, we have found that other lines appeared probably corresponding to the emission from the second kind of Nd^{3+} ions sites.

Figure 7 shows fluorescence spectra of Eu^{3+} in $K_3Sr_2EuNb_{10}O_{30}$. The time resolved spectra consist of broad lines, as in Nd^{3+} emission plots. Indeed, only one wide line representing $^5D_0\rightarrow{}^7F_0$ transition is observed. Therefore, the magnetic dipolar $^5D_0\rightarrow{}^7F_1$ and electric dipolar $^5D_0\rightarrow{}^7F_2$ transitions are of comparable intensity, this implies that Eu^{3+} ions may be distributed in both centrosymmetric and noncentrosymmetric sites. This inhomogeneous broadening can be attributed to the disorder inside the structure evidenced by structural investigation (Table 1).

4 Conclusion

The Sintering and the micropulling down methods have allowed to grow tetragonal tungsten bronze crystals with the general formula $K_3Sr_2LnNb_{10}O_{30}$ (Ln=La, Nd, Sm, Eu, Gd, Er). The refinement of the cationic distribution over the 12- and 15-fold sites, gives rise to two-different crystal chemical formulas depending on the growth technique. The spectroscopic study of trivalent Neodymium and Europium ions in this family shows a broadening of the emission peaks. No evidence of a particular site emission seems to appear for rare earth ions. The inhomogeneous broadening can be attributed to the structural disorder compatible with our structural investigation.

References

1. N.N. Kraink, V.A. Isupov, M.F. Bryzhina, A.I. Agranovskaya, Soviet Phys. Crystal. **9**(3), 281(1964)

2. B.N. Savenka, B. Sangaa, F. Proket, Ferroelectrics **107**, 207(1990)
3. A.M. Glass, J. Appl. Phys. **40**(12), 4699(1969)
4. N. Wakiya, J.-K. Wang, A. Saiki, K. Shinozaki, N. Mizutani, J. Eur. Ceram. Soc. **19**, 1071(1999)
5. H.-F. Cheng, G.-S. Chiou, K.-S. Liu, I.-N. Lin, Appl. Surf. Sci. **113**, /**114**, 217(1997)
6. C. Ting, S. Xiaohong, X. Yuhuan, C. Huanchu, Ferroelectrics **82**, 37(1988)
7. K.S. Singh, R. Sati, R.N.P. Choudhary, J. Mat. Sci. Lett. **11**, 788 (1992)
8. G. Foulon, M. Ferriol, A. Brenier, M.-T. Cohen-Adad, M. Boudeulle, G. Boulon, Opt. Mat. **8**, 65(1997)
9. K. Lebbou, H. Itagaki, A. Yoshikawa, T. Fukuda, F. Carillo-Romo, G. Boulon, A. Brenier, M.T.H. Cohen-Adad, J. Cryst. Growth **210**, 655(2000)
10. A. Brenier, G. Boulon, K. Shimamura, T. Fukuda, J. Cryst. Growth **204**, 145(1999)
11. R.D. Shannon, Acta Crystallogr. **32**, 751(1976)
12. S.M. Pilgrim, A.E. Sutherland, S.R. Winzer, J. Am. Ceram. Soc. **73**, 3122(1990)